Identification of Transverse Band Signature in Satellite Imagery

Annelise Lenz
UW-Madison Cooperative Institute for Meteorological Satellite Studies

ABSTRACT

Transverse bands have commonly been observed in the outflow of thunderstorms, though little literature exists on the subject. The primary objective of this paper is to characterize the transverse band signature in satellite imagery and analyze the relationship to atmospheric turbulence. The transverse band signature was observed in nearly half of all convective systems analyzed between May and August of 2006, commonly in the mature and decay stages of the system. Transverse bands lasted an average duration of 9 hours and generally occurred during the nighttime hours. At least one observation of light (moderate) turbulence was found within transverse bands for 93% (44%) of events, as analyzed through Eddy Dissipation Rate (EDR) observations. Storm size, propagation, and geographic location did not appear to influence transverse bands, though the bands did appear to be associated with negative 300 hPa relative vorticity and positive divergence.

1. Introduction

This paper will focus on one interesting signature in satellite imagery – transverse banding on the edge of a thunderstorm anvil. The transverse band signature in satellite data has not been studied in depth and very little literature exists on the subject, though the occurrence of transverse bands is not an uncommon feature in the life cycle of a thunderstorm. Areas of strong atmospheric turbulence over large regions are often characterized by extensive cloud cover, which sometimes contain well-defined transverse cirrus bands that can be observed in visible or infrared satellite imagery (Ellrod 1985). According to the Federal Aviation Administration (FAA), in-flight turbulence is the leading cause of injuries to airline passengers and flight attendants – approximately 58 people are seriously injured and more than 1,000 minor injuries occur as a result of turbulence in the United States each year (FAA 2008). The improved spatial resolution on both geostationary (GEO) and low-earth orbiting (LEO) satellites allows for the visualization of turbulent mesoscale features such as transverse bands.

This analysis characterizes the frequency of occurrence of this signature from May to August 2006. Multispectral satellite imagery from both GEO and LEO are used to identify the signature and aid in the characterization of the time of occurrence and temporal persistence of the bands. Some upper-air flow patterns associated with transverse bands are identified in an attempt to further understand this signature.

2. Data

2.1 Geostationary Satellite Observations

This study utilizes data from the GOES-12 satellite, which is positioned over the equator at 75°W longitude at an altitude of about 35,800 kilometers, and provides imagery over the Eastern U.S. every 15-30 minutes. This relatively high temporal resolution provides image sequences in which the emergence, evolution, and dissipation of transverse bands can be monitored. GOES-12 collects data in 5 spectral channels in the visible and infrared portion of the electromagnetic spectrum (Menzel and Purdom 1994). For this study, imagery from the following three channels are used: channel 1, measuring radiation in the visible spectral region and having a wavelength of .65 μm (1 μm $=10^{-6}$ meters), channel 3, having a wavelength of 6.7 μm to view the water vapor (WV) content in the mid to upper atmosphere, and channel 4, also known as the infrared (IR) window channel, having a wavelength of 10.7 μm to view infrared cloud and near-surface temperature characteristics.

GOES-12 visible channel imagery has two distinct advantages over the IR window and WV channels. First, visible channel data is collected at a higher spatial resolution than the WV and IR window channel (1 km vs. 4 km), allowing for a clearer depiction of mesoscale features in a convective cloud top. Second, visible imagery displays highlights and shadows in the cloud top, allowing for the visualization of the texture of the top of the cloud and capturing subtle features that are not large enough to show a variation in temperature or water vapor. Thus,

visible imagery is especially useful in the identification of transverse bands. The IR window channel is vital in identifying convective storms with rapidly expanding anvils, especially at night. The WV channel is used to identify turbulent mesoscale features such as transverse bands that do not induce significant fluctuations in the IR window channel temperature pattern.

2.2 Polar-Orbiting Satellite Observations

The Moderate Resolution Imaging Spectroradiometer (MODIS) is an instrument aboard the NASA satellites Terra and Aqua, which are LEO satellites that orbit the earth at 705 kilometers (NASA 2008). The Advanced Very High Resolution Radiometer (AVHRR) is the primary sensor aboard the National Oceanic and Atmospheric Administration (NOAA) LEO satellites that orbit about 850 kilometers above the earth (NOAA 2008). Due to the lower altitude of these satellites, they provide a much higher spatial resolution view of the Earth atmosphere and clouds than geostationary satellites, allowing for the visualization of mesoscale features that are often undetected in the GOES satellite observations. However, each LEO satellite passes over the same non-polar geographic location twice per day, providing far lower temporal resolution than GEO satellites. Thus, GEO and LEO satellite data each have advantages and disadvantages and can be combined to obtain a more complete depiction of turbulence signatures in the satellite imagery.

2.3 Eddy Dissipation Rate Turbulence Observations

Eddy Dissipation Rate (EDR) turbulence observations from commercial aircraft provide an objective measure of the vertical accelerations induced by turbulent atmospheric phenomena. This dataset is produced through the combination of existing sensors, avionics, and communication networks, resulting in a "state of the atmosphere" turbulence diagnostic (Sharman et al. 2006). United Airlines Boeing 737 and 757 aircraft began collecting this EDR data in 1997, recording an observation every minute during flight and automatically transmitting it to the ground. The EDR observing system was designed to provide routine and quantitative measurements of atmospheric turbulence intensity levels, including null observations, addressing many of the deficiencies with pilot reports (PIREPs) (Sharman et al. 2006). EDR observations provide a unique dataset that can be used to study atmospheric turbulence in the transverse band signature.

3. Methodology

The "Summer 2006 Storm Database" (http://www.ssec.wisc.edu/~alenz/Summer2006StormDatabase.html) was developed by identifying transverse banding events from May through August 2006 occurring over the continental United States. To do this, the time evolution of the outflow pattern was monitored for all convection in the time period described above using 4 km IR window GOES infrared imagery. From this analysis, convective cases were identified – a single convective case was defined for both isolated events and events within a system of numerous storms. Multi-storm events were defined by geographic location and time of outbreak – the largest events contained numerous individual storms and covered entire regions of the United States (i.e. the entire Southeast U.S.).

All identified convective events were then analyzed more thoroughly using the GOES visible and IR window imagery to identify whether transverse bands were present. In the case of multi-storm events, each individual storm was analyzed for the existence of transverse bands. Convective cases in which transverse bands did form and were sustained for a significant period of time (at least 30 minutes) were entered into the Summer 2006 Storm Database, where the lifecycle of the storm and transverse band evolution was documented. The EDR dataset was then analyzed for each case in the Summer 2006 Storm Database to determine the nature of the atmospheric turbulence induced by the transverse bands. The Man computer Interactive Data Access System (McIDAS) software package developed by the Space Science and Engineering Center at the University of Wisconsin-Madison was the primary software package used to display, analyze, and manage the data in this study (Lazzara et al. 1999).

4. Analysis of the Transverse Band Signature

4.1 Identification of Bands in Satellite Imagery

Transverse bands do not occur in every convective system that develops, though the banded structures are not entirely uncommon either. For the Summer 2006 Storm Database, 131 convective events were identified between May 1 and August 31. Of

these events, 54 were associated with transverse bands – 41% of the total convective events produced banded structures. Transverse bands can be identified in the visible, IR window, and water vapor channel imagery. The appearance of transverse bands in the IR window and water vapor channels is illustrated in Figure 1 and the visible channel is illustrated in Figure 3. In the visible, bands appear as high cirrus clouds that vary in thickness. The clouds are arranged in long, thin bands that extend away from the storm center, often perpendicular to the storm edge and gravity waves (if present). These cloud signatures are also apparent in the IR window and water vapor imagery, providing good temporal coverage when visible imagery is not available.

Transverse bands are sometimes slightly more difficult to visualize in the GOES IR window imagery due to the reduced spatial resolution. Figure 1 shows the difference between GEO and LEO satellite image resolution for a transverse band case. While the major features of the convective system are depicted sufficiently in the lower resolution GOES imagery, the transverse band signature is much less apparent. For instance, the structures to the east of the system do not appear to be transverse bands at all in the GOES imagery, but are very clearly banded structures when viewed in the AVHRR imagery. Thus, higher resolution IR window data is required to accurately view and identify subtle transverse band signatures in satellite data in the absence of visible imagery. The more robust transverse band signatures can be sufficiently identified in the lower resolution IR window data, as shown on the northern edge of the storm in Figure 1.

Figure 2 depicts cross sections taken through two different sets of transverse bands in the MODIS IR window imagery. In both cross sections the minima in brightness temperatures (individual transverse bands) do not extend more than a few kilometers in length, indicating that the width of an individual transverse band is a meso-γ scale feature. Band separation can vary – spacing between bands can be as small as 1 km and as large as 50 km (analysis not shown), though in most cases bands are generally observed with 5-10 km spacing.

Figure 3 illustrates a comparison of GOES visible and IR window imagery from two different times in a transverse band event. At 1315 UTC the newly developing bands can be detected in the visible imagery but are extremely subtle, if not nonexistent, in the IR window imagery. An hour and a half later, at 1445 UTC, the bands are still nicely depicted in the visible imagery and are beginning to appear in the IR window imagery, specifically along the northern edge of the anvil where the bands begin to extend beyond the rest of the anvil cloud. The bands are difficult to see in the IR window imagery while they are over the anvil cloud due to the small fluctuation in temperature between the bands and anvil, though once the bands extend beyond the anvil cloud the temperature contrast between the clear air and bands is much larger and therefore much more likely to be represented in the IR window imagery.

4.2 Evolution/Emergence

No single factor appeared to be directly related to the formation or lack of transverse bands, though interactions between multiple convective systems appeared to inhibit band sustainability. The ideal case for band production appeared to be a strong, isolated convective system that developed, matured, and dissipated without interacting with any other convective storm. A few cases showed signs of transverse bands earlier in the life cycle of the convective system – near the end of the growth stage and in the beginning of the mature stage, though transverse bands were more commonly observed to emerge near the end of the mature stage of the system and persist through the decay stage of the system. Rapid anvil expansion can sometimes be associated with the production of transverse cloud bands along the periphery of the anvil cirrus cloud. However, transverse bands are not exclusively associated with rapid anvil expansion and rapid anvil expansion does not necessarily produce transverse bands.

Figure 4 illustrates the evolution of banded structures on both the northwest and southeast sides of the storm. Prior to 0515 UTC the storm was intensifying (a general cooling in cloud top brightness temperatures) and was propagating toward the east. At 0515 UTC very small transverse bands begin to emerge from the anvil along the west-northwestern edge. The cloud top brightness temperatures continue to decrease until 0545 UTC, when the bands along the northwestern edge of the anvil become more apparent. After 0615 UTC there is a general warming in the cloud top brightness temperatures, indicating the storm is beginning to decay. As the storm decays bands become more prominent and extend further away from the storm core, though the initial burst

between 0515 UTC and 0545 UTC was the greatest increase in band size and intensity over the entire life cycle. An anticyclonic flow emerges in the anvil cloud pattern, as the large scale mesoscale convective system (MCS) begins to develop its own outflow environment, which acts to govern the rotation and orientation of the bands as the storm begins to rapidly decay around 0745 UTC. As the storm begins to rapidly dissipate, after 0845 UTC, the bands rapidly dissipate as well, as they are already beginning to show signs of decay between the 0815 UTC and 0845 UTC imagery.

Most transverse band cases observed in the Summer 2006 Storm Database involved the emergence of banded structures along the perimeter of the storm; however, a few cases exhibited slightly different behavior. Figure 3 depicts a case in which banded structures appeared to originate in the overshooting top of the storm, right at the core, and extend away from the overshooting top through the anvil, similar to spokes on a wheel. Figure 3 illustrates how these "spoke-like" bands can be traced all the way through the anvil of the storm from the overshooting top out beyond the edge of the anvil. As the storm develops, the bands extend further away from the core of the storm and no longer appear to connect to the overshooting top. The resolution of the GOES IR window imagery is not high enough to distinguish these banded structures from the rest of the anvil, as previously discussed, so it is possible this type of band morphology exists more often than has been observed through this study.

4.3 Geographic Distribution

Transverse bands have been most often observed in convective systems originating in the central U.S. As illustrated in Figure 5, the majority of transverse band events in the Summer 2006 Storm Database occurred in the Great Plains across the Midwestern U.S. These events were generally associated with convective systems that were initiated in the lee of the Rocky Mountains and moved eastward as they developed and dissipated. Figure 5 also depicts a secondary region of transverse band events along the coast of the Gulf of Mexico. A few of the events occurring in the southeastern U.S. and along the Gulf Coast were associated with northward moving tropical disturbances, though many were associated with isolated or multi-storm events.

The geographic distribution of the banded structures with respect to the parent storm is not as easily generalized. Analysis of Figure 5 also indicates the orientation of transverse bands is not determined by storm propagation or the geographic location of the convective system. The majority of storms in the Midwestern U.S. were propagating toward the east, though banded structures seem to form along all sides of the anvil edge, without an apparent preferred direction relative to the parent storm motion. The orientation of banded structures also did not appear to be influenced by the size or shape of the convective system, nor by the speed of storm propagation.

4.4 Temporal Distribution

Transverse bands have been observed at all hours of the day, though are most common during the nighttime hours. Since most transverse bands are observed in the mature and decay stages of convective systems, it follows that bands would most often be observed overnight, as many thunderstorms develop in the late afternoon/evening and generally persist into the early morning hours of the next day. Many cases of transverse bands were observed in which the banded structures persisted for several hours after the original convective system had completely dissipated. In these cases, the banded structures generally detached from the main system during the decay stage and moved away from the dying system, allowing them to maintain the banded cloud structure despite the dissipation of the original convective system.

The analysis of the temporal distribution of transverse bands summarized in Figure 6 was completed by summing the number of times bands were present during the one-hour time intervals. For example, a storm with transverse bands present from 0345 UTC to 0415 UTC would contribute to the total number of band cases in both the 0300-0359 UTC and 0400-0459 UTC time periods. In this way, the total number of cases over the entire graph in Figure 6 is much larger than the number of cases analyzed. Figure 6 depicts a general peak in transverse band presence from approximately 0300 UTC until 1559 UTC, with two local maxima at 0800-0859 UTC and 1400-1449 UTC. A general minimum in band presence can also be inferred from Figure 6, beginning around 1800 UTC and lasting through 0259 UTC.

Also depicted in Figure 6, convective initiation occurs for these band-producing convective systems between the hours of 1700 UTC and 0359 UTC, corresponding with the minimum previously identified in band presence in Figure 6. In fact, 69% of transverse band events from the Summer 2006 Storm Database resulted from storms that developed between the hours of 1800 UTC and 0259 UTC.

The time lag between storm development and the formation of transverse bands ranged from as short as 15 minutes to as long as 14 hours and 45 minutes. Figure 6 illustrates the amount of time that passed between storm initiation and the first emergence of bands, showing an apparent peak of band development 5 to 9 hours after storm initiation. This analysis in Figure 6 disregards the two cases in the Summer 2006 Storm Database that appeared to be tropical cyclones, as these storms developed before moving on shore. The average time lag between storm development and transverse band initiation was 7 hours. From this analysis, one would expect to see the peak in the temporal distribution of transverse bands to occur 5 to 9 hours after the peak in the temporal distribution of storm initiation. The peak in storm initiation occurs around 1800 UTC to 2100 UTC and the peak in transverse bands begins around 0300 UTC, just as expected from the data in Figure 6.

Figure 6 also illustrates the distribution of transverse band duration, peaking around 4-5 hours and again at 8-10 hours. The case in which banded structures lasted 24 hours was a tropical cyclone that made landfall along the Southeast United States; however, the case with bands lasting 20 hours was a convective system over the Midwestern United States. Thus, it is possible to observe bands sustained for a long time in cases other than tropical cyclones. Such a large variability in transverse band duration, along with a fairly long average duration, accounts for such a broad peak in the temporal distribution depicted in Figure 6.

4.5 Turbulence

Transverse bands have proven to be turbulent features through subjective comparison of EDR and satellite imagery. In fact, out of 54 banded events recognized for the Summer 2006 Storm Database, 41 events included at least one flight through the transverse bands. Of these events, 38 (93%) included at least one flight that observed some light turbulence, though some of these events also included flights through the bands that experienced no turbulence at all. Moderate turbulence was observed at least once in 18 of the banded events – 44% of the events with a flight through the bands (analysis not shown).

4.6 Relationship to Upper Level Divergence and Vorticity

The relationship to upper level divergence and vorticity was analyzed for only 33 cases from the Summer 2006 Storm Database (out of 54), limited by the availability of numerical weather prediction model derived divergence and vorticity data in the GOES-8 Satellite Winds Page (located online at http://cimss.ssec.wisc.edu/mesoscale_winds/archive.html). In order to objectively analyze the divergence and vorticity fields, the U.S. Navy's Operational Global Atmospheric Prediction System Model (NOGAPS) forecast wind fields were combined with satellite-derived water vapor winds from the UW-CIMSS algorithm. Derived divergence and vorticity fields are plotted atop GOES water vapor channel imagery, as these were the datasets available for analysis on the aforementioned webpage.

Transverse bands have generally been observed in regions of positive divergence at 300 hPa, an example of which is illustrated in Figure 7. From the cases with model data described above, 91% had bands form in a region of positive divergence; 76% of cases had bands form in a gradient of divergence, which was usually due to a local maximum of divergence located over the storm center, and 24% of cases had bands form in a local maximum of positive divergence.

Transverse bands were also generally observed in regions of negative relative vorticity at 300 hPa; 97% of cases had bands form in a region of negative relative vorticity. The most common location for the bands to form was in a region of a strong relative vorticity gradient, which occurred in 82% of the cases (Figure 7); 21% of cases had bands form in a local minimum of relative vorticity and 9% of cases had bands form parallel to lines of constant negative relative vorticity. This analysis was done using all sets of bands, as some cases had two or more sets of bands developing in different relative vorticity fields (i.e., one case formed band in a local minimum of relative vorticity and in a gradient of negative relative vorticity). In the event of more than one set of bands in different relative vorticity fields, cases were counted twice – once in each category.

The case illustrated in Figure 7 represents the majority of cases studied, as there is a local minimum of relative vorticity positioned over the center of the storm with the bands forming in the strongest gradient. The bands also formed in a gradient of divergence due to the largest values of divergence also occurring at the center of the storm. The bands illustrated in Figure 7 persist hours after the storm dissipates, extending in a north-south direction initially and tilting toward a northeast-southwest orientation over time. The bands appear to follow the relative vorticity gradient, changing orientation in order to remain parallel to the relative vorticity gradient vector and propagating to remain within the region of the strongest gradient. From Figure 7 it is apparent that the bands remain in a region of positive divergence throughout their life cycle, though the structure and distribution of divergence is not temporally consistent.

The majority of banded structures form in a region of a strong relative vorticity gradient, though the bands do not always favor the strongest gradient present (analysis not shown). Also, the existence of a strong relative vorticity gradient does not guarantee the survival of transverse bands. Figure 8 depicts a case in which a convective system produces transverse bands over Wisconsin around 1145 UTC. The bands move east more quickly than the decaying system and finally dissipate over New York. These bands do not form in a strong gradient of relative vorticity, but eventually move in the gradient depicted in Figure 8. However, once the bands move into the gradient, they remain in the gradient oriented parallel to the gradient vector until they dissipate. Despite the increase in the gradient between 1745 UTC and 1945 UTC, the bands almost completely dissipate by 1945 UTC. Also interesting to note is the divergence – the bands dissipate in a region of positive divergence.

From this analysis it is apparent that, while generalizations can indicate possible behavior for transverse bands, the environmental characteristics associated with banded events are highly variable. A strong gradient of relative vorticity does not guarantee the development or sustainability of transverse bands. Positive divergence appears well correlated with band development, but does not guarantee the sustainability of transverse bands either. Also, the model derived vorticity and divergence fields were not always temporally co-located with the satellite imagery, so some mismatch may have occurred in the above analysis. Due to the variable nature of transverse bands, generalizations can guide initial analysis but will not always accurately predict the behavior of transverse bands.

5. Conclusion

Transverse bands were observed to be long-lived and occurred in the mature and decaying stages of nearly half of all convective systems initiated; bands were commonly observed over night. The average lag time between storm initiation and band formation was about 7 hours and the average duration of the bands was about 9 hours. In most cases, transverse bands appeared to originate at the storm edge in the outflow of the convective system, though some cases exhibited evidence for the production of banded structures earlier in the storm lifecycle closer to the storm core. The bands have been observed primarily in the Great Plains and Midwest, though were also not uncommon along the Gulf Coast. Nearly every case of transverse bands was associated with at least light turbulence, and just less than half of the cases were associated with moderate or greater turbulence. The orientation of transverse bands did not appear to be influenced by storm size, propagation, or geographic location, though the bands did appear to be associated with the upper level dynamics as represented by NWP model output. Almost every case of transverse bands originated in a region of negative relative vorticity and positive divergence. Most cases produced bands in the gradient of relative vorticity, which appeared to sustain the bands beyond the life of the storm in some cases.

The increased spatial and temporal resolution of future satellite imagery will greatly enhance the understanding of all mesoscale atmospheric features, especially transverse bands. As other airlines obtain EDR capabilities, the EDR dataset will become more complete, and thus more useful for the study of turbulence associated with mesoscale satellite signatures. These future tools will prove to be an invaluable resource to the ongoing research of transverse bands in the outflow of thunderstorms.

6. References

Ellrod, G. P., 1985: Detection of high level turbulence using satellite imagery and upper air data. NOAA Tech. Memo. NESDIS 10, U.

S. Dept. Of Commerce, Washington, DC, 30pp.

Federal Aviation Administration (FAA), cited 2008: Turbulence: Staying Safe. [Available online at http://www.faa.gov/passengers/fly_safe/turbulence/.]

Lazzara M. A., and Coauthors, 1999: The Man computer Interactive Data Access System: 25 Years of Interactive Processing. *Bull. Amer. Meteor. Soc.*, **80**, 271-284.

Menzel, W.P., and J.F. Purdom, 1994: Introducing GOES-I: The First of a New Generation of Geostationary Operational Environmental Satellites. *Bull. Amer. Meteor. Soc.*, **75**, 757–781.

National Aeronautics and Space Administration (NASA), cited 2008: MODIS Web. [Available online at http://modis.gsfc.nasa.gov/about/.]

NOAA Satellite and Information Service, NESDIS, cited 2008: Geostationary Satellites. [Available online at http://www.oso.noaa.gov/goes/index.htm.]

Sharman, R., L. Cornman, J. K. Williams, S. E. Koch, and W. R. Moninger, 2006: The FAA AWRP Turbulence PDT, *12th Conference on Aviation Range and Aerospace Meteorology*, Atlanta, GA, Amer. Meteor. Soc., 3.3.

7. Figures

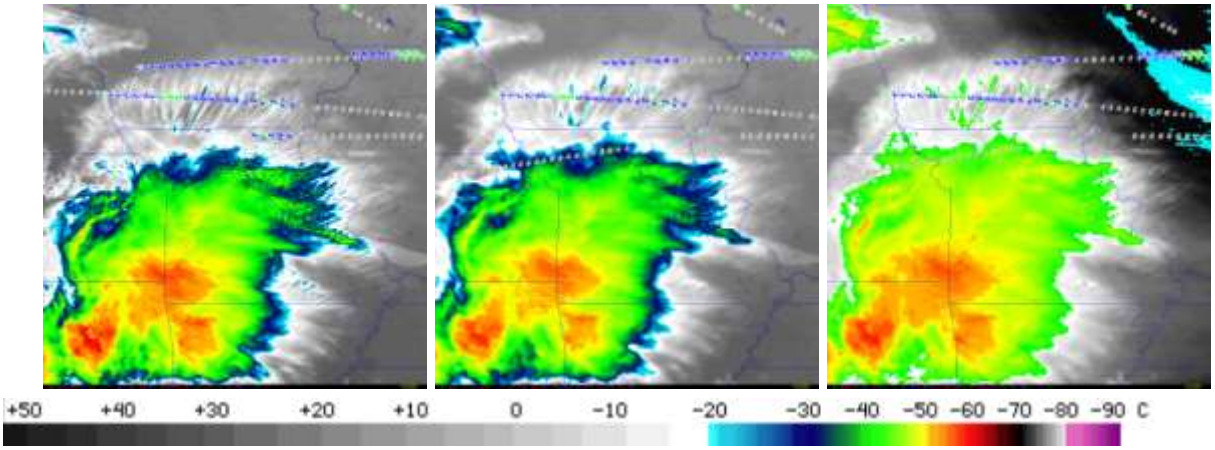

Figure 1: AVHRR IR window image at 0905 UTC (left), GOES IR window image at 0915 UTC (middle), GOES WV image at 0915 UTC (left) from June 16, 2005 over Missouri.

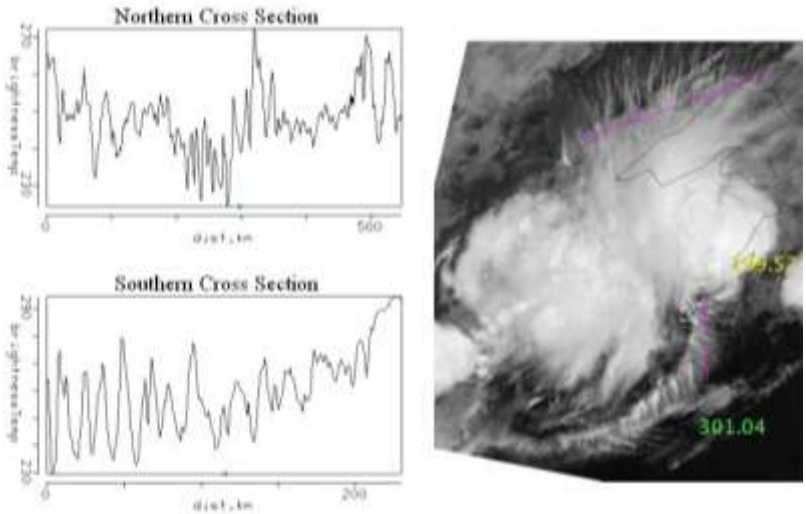

Figure 2: Cross sections through northern (top) and southern (bottom) transverse bands on left, MODIS IR window imagery from 0800 UTC on August 2, 2006 on right. Locations of cross sections are identified on MODIS image by purple lines with the center point defined by the green square (shown on both MODIS image and cross sections).

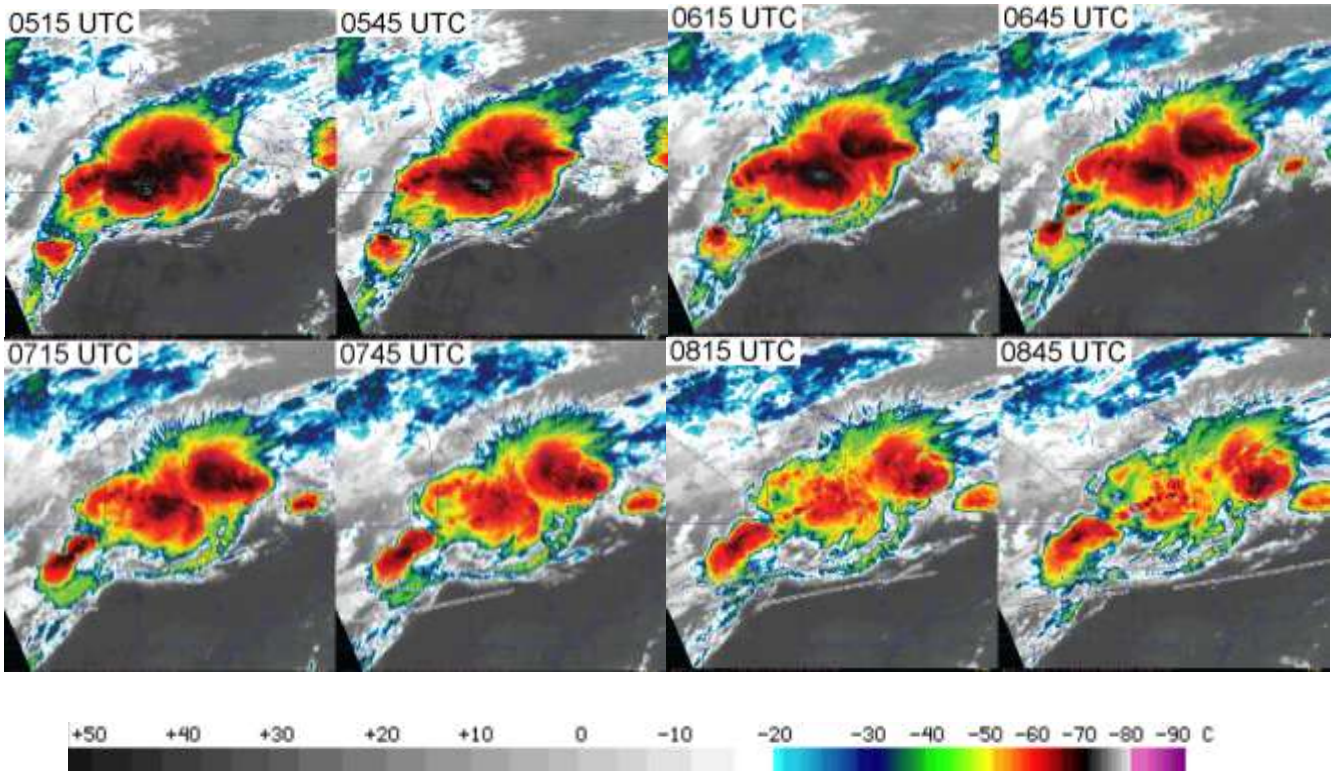

Figure 3: GOES visible and IR window imagery from July 19, 2006 at 1315 UTC (left) and 1445 UTC (right) over Minnesota.

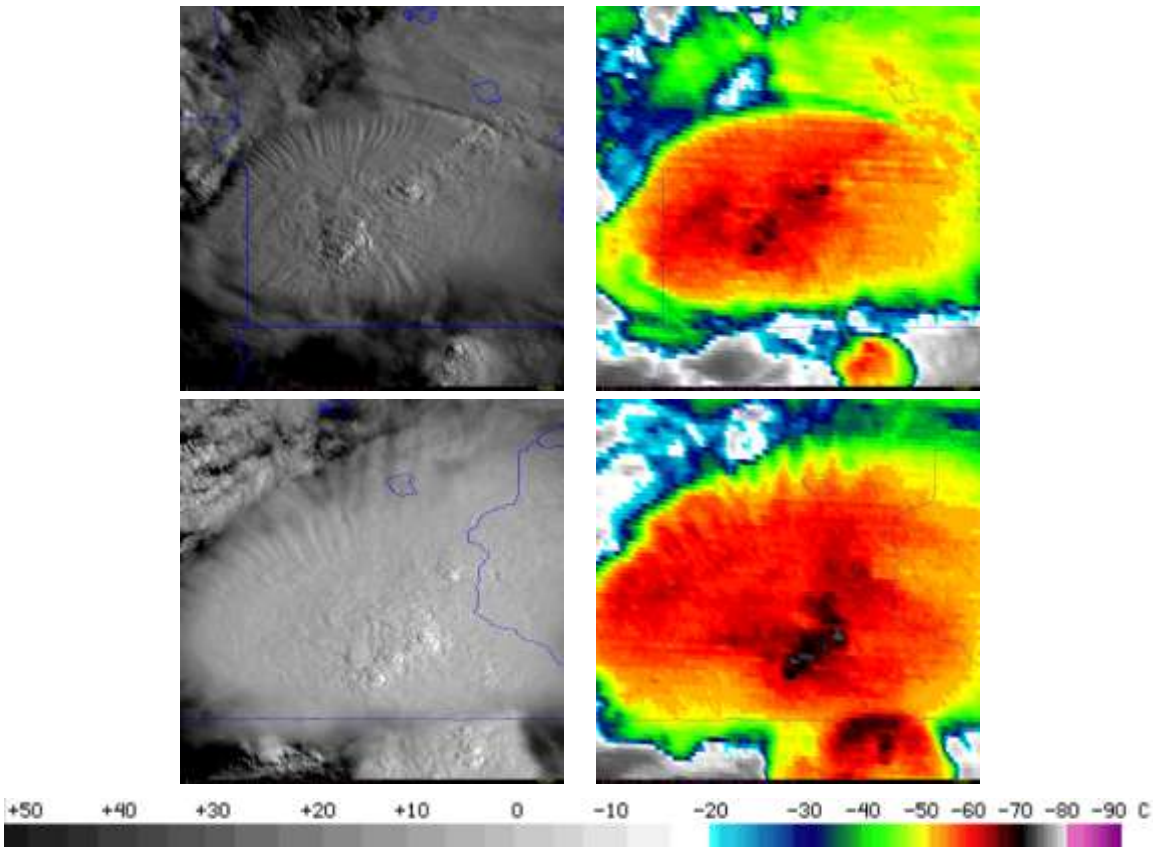

Figure 4: Evolution of on August 2, 2006. Images are taken every 30 minutes from 0515 UTC through 0845 UTC over Minnesota and Wisconsin from GOES IR window imagery.

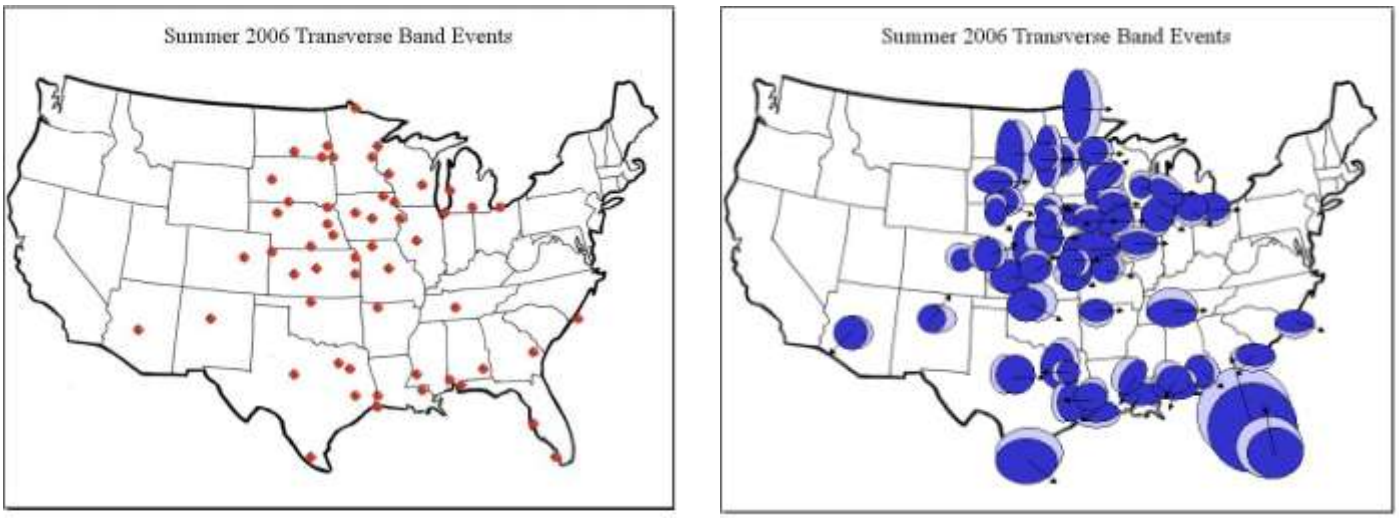

Figure 5: Geographic distribution of transverse band events - red dots represent the location of the storm center at the time when transverse bands first appeared (left), dark blue circles represent the location of the anvil, light blue circles represent the location of the bands, and black arrows indicate direction of storm propagation and are coarsely proportional to the speed of the convective system.

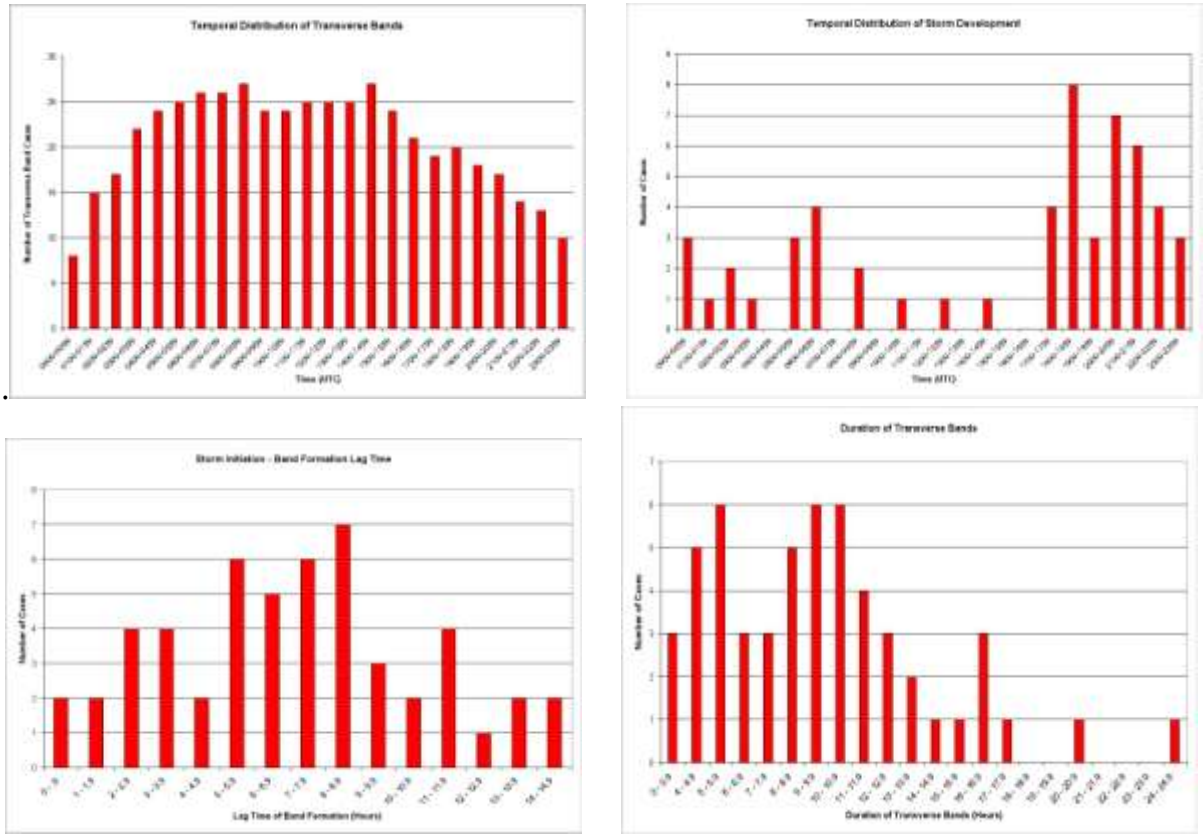

Figure 6: Bar graphs showing the temporal distribution of transverse bands (top left), storm development (top right), time lag between storm initiation and transverse band formation (bottom left), and transverse band duration (bottom right).

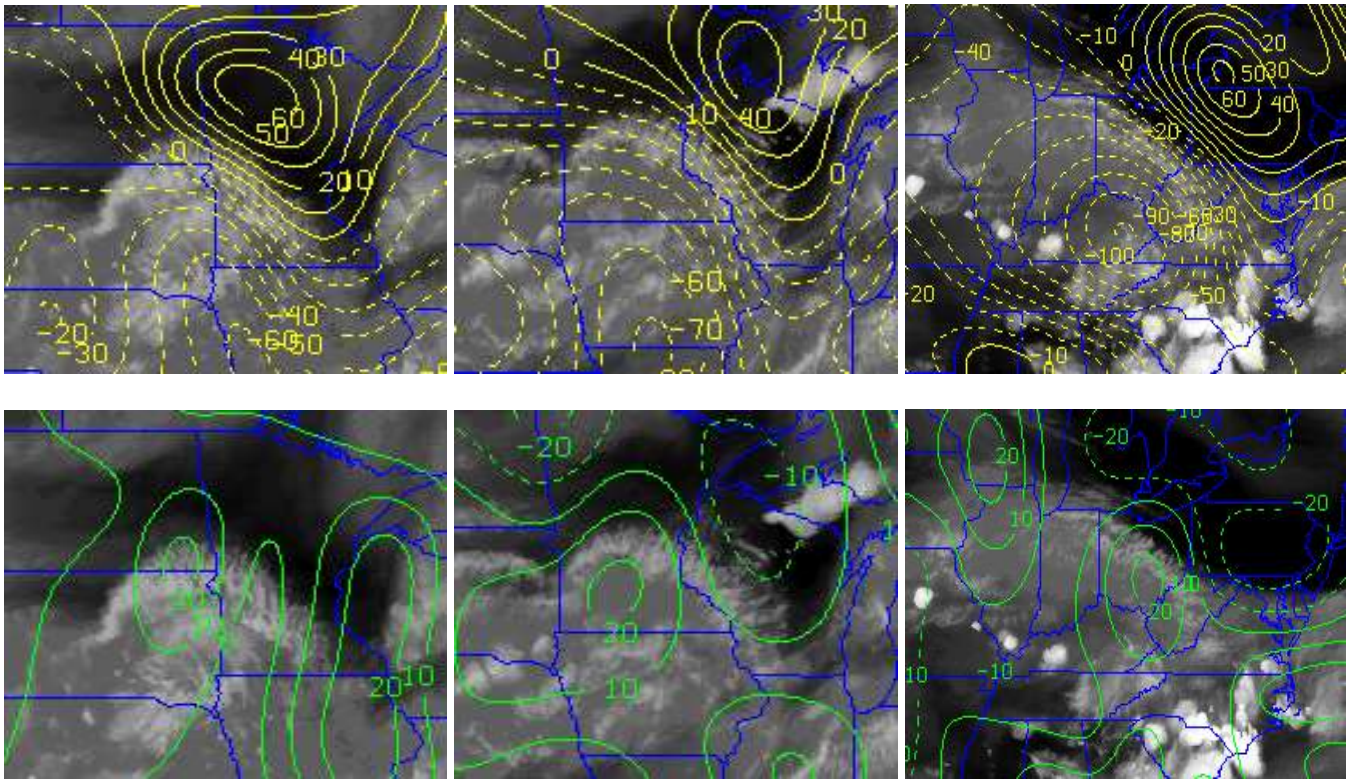

Figure 7: 300 hPa relative vorticity (top) and divergence (bottom) plotted on GOES water vapor imagery on July 1, 2006 at 1245 UTC (left), 1545 UTC (middle), and 1915 UTC (right).

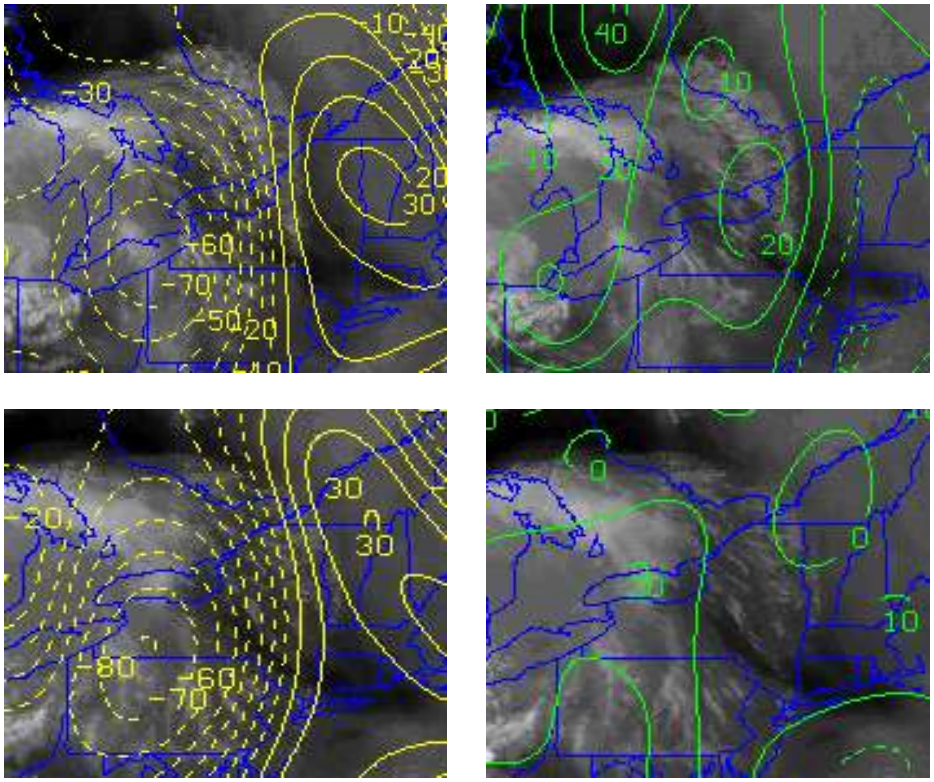

Figure 8: 300 hPa relative vorticity (left) and divergence (right) plotted on GOES water vapor imagery on August 6, 2006 at 1745 UTC (top) and 1945 UTC (bottom).